

Cortical Pathology in Multiple Sclerosis Detected by the T1/T2-Weighted Ratio from Routine Magnetic Resonance Imaging

Ruthger Righart, MD,^{1,2} Viola Biberacher, MD,^{1,2} Laura E. Jonkman, PhD,³
 Roel Klaver, PhD,³ Paul Schmidt, PhD,^{1,2,4} Dorothea Buck, MD,¹
 Achim Berthele, MD,¹ Jan S. Kirschke, MD,⁵ Claus Zimmer, MD,⁵
 Bernhard Hemmer, MD,^{1,6} Jeroen J. G. Geurts, PhD,³ and Mark Mührlau, MD^{1,2}

Objective: In multiple sclerosis, neuropathological studies have shown widespread changes in the cerebral cortex. In vivo imaging is critical, because the histopathological substrate of most measurements is unknown.

Methods: Using a novel magnetic resonance imaging analysis technique, based on the ratio of T1- and T2-weighted signal intensities, we studied the cerebral cortex of a large cohort of patients in early stages of multiple sclerosis. A total of 168 patients with clinically isolated syndrome or relapsing–remitting multiple sclerosis (Expanded Disability Status Scale: median = 1, range = 0–3.5) and 80 age- and sex-matched healthy controls were investigated. We also searched for the histopathological substrate of the T1/T2-weighted ratio by combining postmortem imaging and histopathology in 9 multiple sclerosis brain donors.

Results: Patients showed lower T1/T2-weighted ratio values in parietal and occipital areas. The 4 most significant clusters appeared in the medial occipital and posterior cingulate cortex (each left and right). The decrease of the T1/T2-weighted ratio in the posterior cingulate was related to performance in attention. Analysis of the T1/T2-weighted ratio values of postmortem imaging yielded a strong correlation with dendrite density but none of the other parameters including myelin.

Interpretation: The T1/T2-weighted ratio decreases in early stages of multiple sclerosis in a widespread manner, with a preponderance of posterior areas and with a contribution to attentional performance; it seems to reflect dendrite pathology. As the method is broadly available and applicable to available clinical scans, we believe that it is a promising candidate for studying and monitoring cortical pathology or therapeutic effects in multiple sclerosis.

ANN NEUROL 2017;82:519–529

Traditionally, multiple sclerosis (MS) has been regarded as an inflammatory disease of the central nervous system characterized by demyelinated lesions in the white matter (WM). Yet several lines of evidence indicate that the spectrum of MS pathology is much broader, including cortical pathology.^{1–3} This concept is supported by studies on postmortem brain tissue,^{1,3} brain biopsies,⁴ and magnetic resonance imaging (MRI). Most

of these studies focused on cortical demyelinated lesions, which can be visualized by high-field MRI.⁵ Furthermore, cortical demyelination correlates with a decrease in the magnetization transfer ratio (MTR), and about 18% of the cortical demyelinated lesions go along with an intensity increase in double inversion recovery images.^{6,7} Moreover, cortical demyelination is a functionally relevant aspect of tissue damage in MS; it is associated with

View this article online at wileyonlinelibrary.com. DOI: 10.1002/ana.25020

Received Oct 21, 2015, and in revised form Jun 20, 2017. Accepted for publication Jun 22, 2017.

Address correspondence to Dr Mührlau, Department of Neurology, Technische Universität München, Ismaningerstr. 22, D-81675 Munich, Germany.
 E-mail: mark.muehlau@tum.de

From the ¹Department of Neurology, Rechts der Isar Hospital, Technical University of Munich, Munich, Germany; ²TUM Neuroimaging Center, Rechts der Isar Hospital, Technical University of Munich, Munich, Germany; ³Department of Anatomy and Neurosciences, VU University Medical Center, Amsterdam, the Netherlands; ⁴Department of Statistics, Ludwig Maximilian University of Munich, Munich, Germany; ⁵Department of Neuroradiology, Rechts der Isar Hospital, Technical University of Munich, Munich, Germany; and ⁶Munich Cluster for Systems Neurology (SyNergy), Munich, Germany

cognitive deficits^{8,9} and with a higher risk for transition from the relapsing–remitting to the secondary progressive phase of MS.¹⁰ However, cortical pathology seems to extend beyond the area of demyelinated lesions. Histological studies demonstrated transected neurites not only in axons within demyelinated lesions but also in dendrites within the myelinated cortex,¹¹ and a recent study demonstrated loss of dendritic spines independent of cortical demyelination and axon loss.²

Recently, an MRI-based method to study the tissue properties of the cerebral cortex was introduced. This method is based on the ratio of T1- and T2-weighted (w) image signal intensities.¹² Heretofore, the histological substrate has been unclear, although myelin content has been suggested based on indirect evidence.^{12–14} Yet 3 features of this method are particularly attractive for MS research: (1) with regard to precision, it seems to enable mapping of human cortical areas across the whole brain; (2) with regard to feasibility, it can be applied to large cohorts of patients and it is based on the ratio of intensity values from 2 conventional sequences, namely the T1w and T2w sequences, which are part of many clinical MRI protocols; and (3) with regard to functional relevance, its measures have been described to be related with performance variability in normal subjects.¹⁵

In the current study, we pursued 2 goals: (1) in early MS, we aimed to map the cortical T1w/T2w ratio by comparing a group of patients to a group of healthy controls (HC) and to evaluate whether these changes are functionally relevant by correlating them with clinical scores; and (2) we tested the commonly held view that the cortical T1w/T2w ratio reflects myelin by combining postmortem imaging and histopathology of MS brain donors.

Subjects and Methods

Subjects, Acquisition, Processing, and Statistical Analysis of In Vivo MRI

The study was performed in accord with the declaration of Helsinki and approved by the local ethics committee of the medical faculty of the Technical University of Munich (TUM). Patients were recruited from the in-house observation study called TUM-MS, and data were derived from routine yearly follow-up visits. Aiming at the earlier MS stages of clinically isolated syndrome (CIS) and relapsing–remitting MS, we included all patients with at least 1 demyelinating attack, a minimal interval to the last demyelinating attack of 4 weeks, a minimal interval to last steroid administration of 2 weeks, at least 2 brain WM lesions typical for MS, and a score on the Expanded Disability Status Scale (EDSS) < 4.¹⁶ Further protocol-conforming MRI data (see below) as well as complete clinical and neuropsychological testing—all acquired within 2 weeks—had to be available. This group initially comprised 186 patients. Eighteen

MRI datasets were excluded for technical reasons (see below). Demographic and clinical parameters of the remaining 168 patients are given in Table 1. We will refer to this group as the MS group, although 28 patients had CIS. Of these, 23 fulfilled the criteria for dissemination in space.¹⁷ The types of clinical manifestation were optic neuritis (n = 10), sensory symptoms (n = 11), and others (optic neuritis and sensory symptoms, brachiofacial paresis, hemiparesis, monoparesis of the left leg, disturbance of fine motor skills in the left arm, quadrantanopia, oculomotor disturbance); the mean duration between the demyelinating attack and MRI was 1.3 years (median = 0.8, standard deviation [SD] = 1.5, range = 0.1–5.6). We compared the MS group to a group of 83 age- and sex-matched HC. Controlling for age-related effects seemed mandatory. On the one hand, we expected an MS-related decrease of the T1w/T2w ratio most likely resulting from an age-related decrease, given that older patients are on average more severely affected than younger patients. On the other hand, the T1w/T2w ratio was reported to increase by 1% per year between 18 and 35 years of age,¹⁸ which seems to continue to the early 50s, followed by a decline in the late 50s.¹⁵ MRI datasets of 3 HC had to be excluded for technical reasons (see below). We will refer to the group of the remaining 80 HC as the HC group. MRI data of the HC group were taken from our in-house database of HC. Subjects included in this database were either scanned in the context of other imaging studies at TUM Neuroimaging Center as HC (n = 31) or in the context of medical examinations (n = 49) performed because of transient headache or symptoms that retrospectively could not be related to a severe or chronic neurological disorder (eg, transient sensory symptoms due to mechanical irritation of a peripheral nerve). Selection was exclusively driven by age and sex comparable to the MS group and availability of MRI data with exactly the same sequences described below.

In the context of TUM-MS, we follow a large cohort of MS patients. The following clinical scores are obtained yearly: EDSS,¹⁹ Multiple Sclerosis Functional Composite,²⁰ Beck Depression Inventory II,²¹ and the Multiple Sclerosis Inventory Cognition (MuSIC),^{22,23} which is broadly used in Germany and also applied to the German national cohort study of the Competence Network Multiple Sclerosis. MuSIC consists of 5 subtests to assess the cognitive core deficits in MS: attention and memory are tested first by Wordlist A (immediate recall of 10 spoken words performed twice), second by Wordlist B (immediate recall of 10 spoken words performed once, now also assessing set-shifting capacity), and third by Wordlist A Delayed (delayed recall of Wordlist A performed once later during the testing); mental set shifting and cognitive information speed processing are tested by Verbal Fluency (alternating naming of terms belonging to 2 different categories within 1 minute); inhibitory control is captured by a Stroop test called Interference; fatigue is covered by a short questionnaire. Demographic and clinical data including disease-modifying drugs are summarized in Table 1.

All subjects underwent magnetic resonance scanning with the same 3T scanner (Achieva; Philips, Best, the Netherlands)

TABLE 1. In Vivo Magnetic Resonance Imaging Cohort

Characteristic	HC	MS
No.	80	168
Age, yr, mean (range)	30.8 (18.6–48.8)	30.8 (19.1–39.2)
Sex, M/F, No. [%]	26/54 [33/67]	53/115 [32/68]
CIS/RRMS	NA	28/140
Disease duration, yr, mean/median/range	NA	3.5/2.6/0.11–15.12
Disease-modifying therapy, No.	NA	IFN, 63; GA, 26; Nat, 7; Fin, 8; none, 62
EDSS, median, range	NA	1.0, 0–3.5
MSFC, mean, range	NA	0.6, –0.7 to 1.6
BDI, mean/range/mild/moderate/severe depression	NA	6.0/0–43/8%/2%/1%
MuSIC fatigue, mean/range/fatigued	NA	7.2/3–19/23%
MuSIC cognition, mean, range, mild, moderate, severe cognitive impairment	NA	25.4/10–30/7%/2%/1%
Lesion volume, ml, mean \pm SD	NA	3.8 \pm 6.2

BDI = Beck Depression Inventory II; CIS = clinically isolated syndrome; EDSS = Expanded Disability Status Scale; F = female; Fin = fingolimod; GA = glatiramer acetate; HC = healthy controls; IFN = interferon beta-1a/b; M = male; MS = multiple sclerosis; MSFC = Multiple Sclerosis Functional Composite; MuSIC = Multiple Sclerosis Inventory Cognition; NA = not applicable; Nat = natalizumab; RRMS = relapsing–remitting MS; SD = standard deviation.

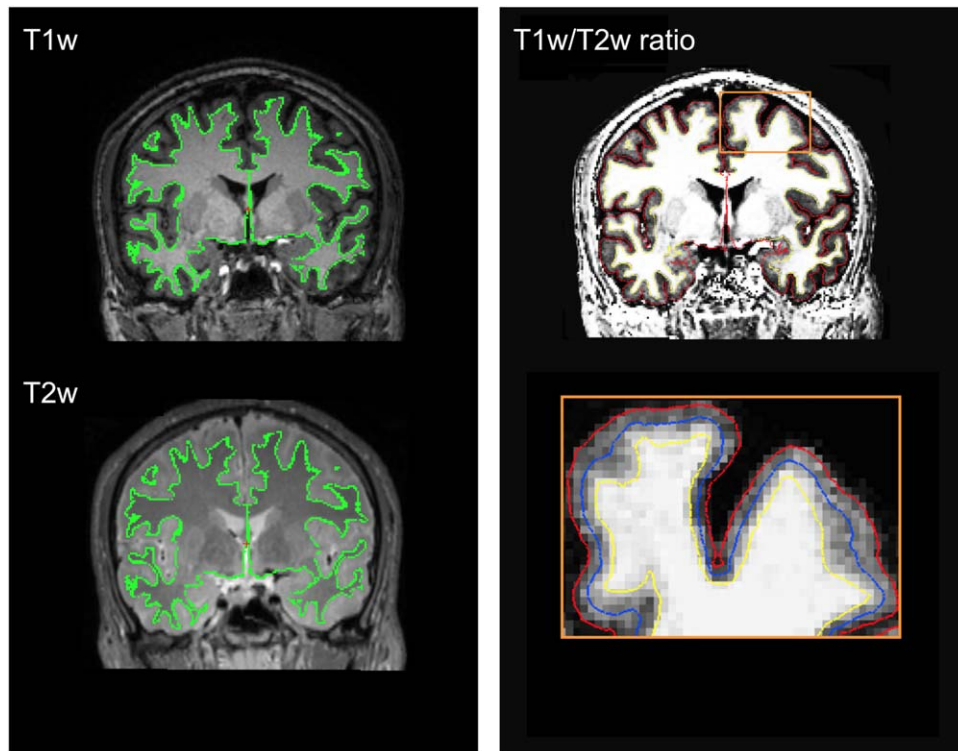


FIGURE 1: Method of T1/T2-weighted (w) ratio maps. T1w and T2w scans (left panel) are registered using *bbregister* (as implemented in the *FreeSurfer* software package), which uses the white matter surfaces (*green line*) to register the cortical surfaces. T1w/T2w ratios are estimated by dividing the T1w by the T2w image (right panel). The T1w/T2w ratio values are sampled on the midthickness surface (*blue line*, right panel), which is positioned halfway in-between the white matter surface (*yellow line*) and cortical pial surface (*red line*).

and the same protocol. The 3-dimensional (3D) gradient-echo T1w sequence used magnetization-prepared 180° radio-frequency pulses and rapid gradient-echo sampling with a spatial resolution of $1.0 \times 1.0 \times 1.0\text{mm}^3$, a repetition time (TR) of 9 milliseconds, an echo time (TE) of 4 milliseconds, and a flip angle of 8° . The T2w sequence had a spatial resolution of $1.0 \times 1.0 \times 1.5\text{mm}^3$, a TR of 4,000 milliseconds, a TE of 35 milliseconds, and a flip angle of 90° . For the segmentation of WM lesions, we also acquired a 3D fluid-attenuated inversion recovery sequence with a spatial resolution of $1.0 \times 1.0 \times 1.5\text{mm}^3$, a TR of 10,000 milliseconds, a TE of 140 milliseconds, and a time to inversion of 2,750 milliseconds.

The main idea of mapping the cortical ratio of the T1w and T2w signal was 2-fold¹²: (1) by dividing the T1w by the T2w signal value, quantification of the signal intensity becomes possible to some degree, as this procedure levels off the bias field and scales the image intensity; as a result, the T1w/T2w ratio constitutes a potential marker of cortical tissue integrity independent of atrophy; and (2) although indirect, there is evidence that the T1w signal of both cerebral WM and cortex mainly results from myelin.^{12,24,25}

T1w images were processed using the software package FreeSurfer 5.3 (<http://surfer.nmr.mgh.harvard.edu>), performing brain extraction, intensity normalization, automated tissue segmentation, surface-based analysis of cortical thickness, generation of the WM surface and pial surface, surface topology correction, automated whole brain segmentation, and spherical interindividual surface alignment.^{26,27} The T2w image was registered to the T1w image using FreeSurfer's `bbregister`, which performs within-subject registration using a boundary-based cost function.²⁸ Given the cortical segmentation of one image (T1w), this routine processes images of different modalities and resolutions through resampling of the images by trilinear interpolation, resulting in images with the standard resolution of FreeSurfer ($1 \times 1 \times 1\text{mm}^3$). Manual WM surface topology correction was performed thoroughly as was visual control of the coregistration of T1w and T2w images (Fig 1). We did not encounter problems in the vast majority of cases. Juxta- and leukocortical lesions that we identified on the T1w anatomical surfaces and that disturbed the cortex segmentation were accounted for by manual correction of WM topology (ie, adding voxels of these lesions to WM volume, also referred to as filling) and rerunning the pipeline. Yet we had to exclude datasets from 18 patients and from 3 HC; WM lesions severely disturbed the cortical segmentation in 13 patients, and registration between the T1w and T2w scans was inaccurate in 5 patients and 3 HC. The T1w/T2w ratio values were sampled at the midthickness surface, which is halfway between the WM and gray matter (GM) surface, by using the `mri_vol2surf` tool. This provides midthickness surface maps of the T1w/T2w ratio. In line with previous work,¹² we will refer to these images as T1w/T2w ratio maps.

The total WM lesion volume was measured by the lesion growth algorithm as implemented in our lesion segmentation

TABLE 2. Clinical Correlations with the T1/T2-Weighted Ratio in the Posterior Cingulate

Tests	Subtests	Pearson <i>r</i>	Unadjusted <i>p</i>
EDSS		-0.15	0.05
MSFC	25-foot walk test	-0.09	0.25
	9-hole peg test	-0.16	0.03
	PASAT	0.08	0.28
MuSIC	Wordlist A	0.16	0.04 ^a
	Wordlist B	0.25	0.001 ^a
	Verbal Fluency	0.08	0.29
	~Mistakes	0.07	0.36
	Interference	-0.10	0.20
	Wordlist A Delayed	-0.04	0.64
	Fatigue	-0.14	0.06
Depression	BDI	-0.07	0.34

^aBonferroni corrected $p < 0.05$.

BDI = Beck Depression Inventory II; EDSS = Expanded Disability Status Scale; MSFC = Multiple Sclerosis Functional Composite; MuSIC = Multiple Sclerosis Inventory Cognition; PASAT = Paced Auditory Serial Addition Test.

tool (default settings, version 1.2.3),²⁹ which is freely available (www.statistical-modeling.de/1st.html).

To compare the overall cortical T1w/T2w ratio of the MS group to that of the HC group, we calculated the individual means of T1w/T2w ratio values across the cerebral cortex and compared the two groups by the *t* test. To investigate region-specific group differences, a vertexwise general linear model was run across the T1w/T2w ratio maps for a total of 163,842 vertices per hemisphere. We applied a false discovery rate (FDR) of < 0.05 to correct for multiple comparisons. In a second step, we applied the more conservative threshold of $p < 0.00001$ uncorrected to visualize areas of most reduced T1w/T2w ratio values. Peak coordinates of significant clusters were determined using FreeSurfer Talairach coordinates based on a nonlinear transform from MNI305 space. We extracted cluster values to perform Pearson correlation analyses with each of the 12 clinical and neuropsychological parameters given in Table 2. We chose this strategy to circumvent whole brain correlation analyses with all 12 clinical scores, which would have resulted in a very conservative and, hence, less sensitive approach given the necessity to correct for multiple testing across both the brain and clinical scores. In further analyses, we extended the simple correlations to partial correlations by including age, global cortical thickness, and WM lesion volume as nuisance variables to exclude a substantial influence of these variable on our results.

In the last part of the analyses of our in vivo MRI data (validation of the T1w/T2w ratio), we tested whether our T1w/

TABLE 3. Demographic and Clinical Parameters of MS Brain Donors

Patient	Age, yr	Gender	Postmortem Delay, h	MS Type	Disease Duration, yr	Cause of Death
1	51	M	4.0	SPMS	20	Pneumonia
2	57	F	3.5	SPMS	25	Euthanasia
3	86	M	3.5	SPMS	61	Pneumonia
4	56	M	5.0	SPMS	14	MODS
5	53	M	4.0	SPMS	25	Euthanasia
6	56	F	4.0	SPMS	32	Pneumonia
7	80	M	4.5	SPMS	45	Pneumonia
8	70	M	4.0	PPMS	26	MODS
9	84	F	3.3	SPMS	50	Euthanasia

F = female; M = male; MODS = multiple organ dysfunction syndrome; MS = multiple sclerosis; PPMS = primary progressive multiple sclerosis; SPMS = secondary progressive multiple sclerosis.

T2w ratio maps behaved as expected with regard to (1) spatial distribution across the brain, (2) age-related increase, and (3) independence of cortical thickness. First, we visually compared our T1w/T2w ratio maps to those reported recently.¹² Second, age-related effects of whole surface estimates were analyzed, as previous MRI studies had observed an increase until the age of 50 years, followed by a decline in the late 50s.^{18,30} We applied a linear regression model to estimate the relation to age. Analysis of variance (ANOVA) was used to assess interaction effects between group and age. Third, we tested whether the T1w/T2w ratio values are unique measures rather than a poor reflection of the cortical thickness. Pearson correlation coefficients between cortical thickness and T1w/T2w ratio values were computed in a vertexwise manner across all subjects separately for the HC group and the MS group.

Statistical significance of all results is indicated by 2-sided *p* values.

Postmortem MRI and Histopathology

The study was approved by the institutional ethics review board of VU University Medical Center. The detailed methodology has been described recently.^{31,32} Only autopsies with very short postmortem delay (≤ 7 hours) were included. Eleven patients were available with a T1w and a T2w MRI sequence, which were processed like the in vivo MRI images. Because of severe atrophy, we could not process the MRI datasets of 2 patients; the characteristics of the remaining 9 patients are given in Table 3. Regions of interest (ROIs) were determined according to the Aparc atlas as implemented in FreeSurfer,³³ and corresponded to the available tissue blocks from the 5 left hemispheric ROIs of the inferior frontal gyrus, superior frontal gyrus, anterior cingulate gyrus, inferior parietal gyrus, and superior temporal gyrus. Tissue blocks were excluded if they contained macroscopic MS lesions or MS lesions visible in the double inversion recovery sequence.³⁴ Hence, only normal-appearing GM was sampled as part of the standardized autopsy procedure. In the

normal-appearing cortical GM, myelin, axons, and dendrites were measured in relative optical density units.³² We also determined the average cortical thickness per tissue block.³¹ Respective numbers of tissue blocks available for each measurement were 36 (myelin), 36 (axons), 35 (dendrites), and 37 (cortical thickness). Consecutive sections were stained as previously described.³⁵

Generalized estimating equations (GEEs) were used to analyze the relationship between histopathological measurements (average per tissue block) and the T1w/T2w ratio (average of vertices per respective ROI). As a control analysis, we also investigated the relationship between cortical thickness values derived from histology and those derived from MRI. GEEs take into account that the outcome variable was measured in different brain areas within one patient (nestedness). GEEs also work with unbalanced designs, that is, when missing data occur at random. Accordingly, it has already proved useful in a similar context, namely for the analysis of the histopathological substrate of cortical atrophy in MS.³² One GEE analysis was run per histopathological measurement as explanatory variable. All variables were scaled (*z*-transformed) prior to analysis to achieve comparability between estimated effect sizes.

T1w/T2w Ratio of the Posterior Cingulate Cortex across Groups In Vivo and Postmortem

We investigated whether T1w/T2w ratio values in the posterior cingulate cortex are lower in late stage MS compared to patients in earlier stages and to HC. The ROI of the posterior cingulate cortex was taken from the 2 clusters derived from the comparison of the MS group and HC group at the uncorrected *p* value of 0.0001. Vertex values were averaged across this ROI per subject. As data were acquired from different scanners with different sequences, we scaled the ROI values with the average across the whole cortex per subject. These values were then plotted and compared across groups.

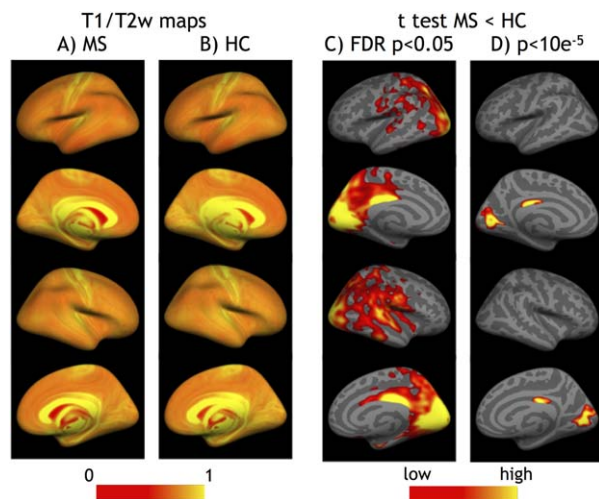


FIGURE 2: In vivo cortical T1w/T2w-weighted (w) ratio maps. (A, B) Group-averaged T1w/T2w ratio maps of the multiple sclerosis (MS) and healthy control group (HC). (C, D) Statistical maps of the difference between the MS and HC groups using a false discovery rate (FDR) of <0.05 (C) and the very conservative threshold of $p < 0.00001$ uncorrected (D) indicate a widespread decrease of the T1w/T2w ratio with a preponderance of posterior regions (C) peaking in the posterior cingulate and primary visual cortex (D). Images are scaled from dark red to light yellow as indicated by the bars at the bottom.

Results

In Vivo MRI

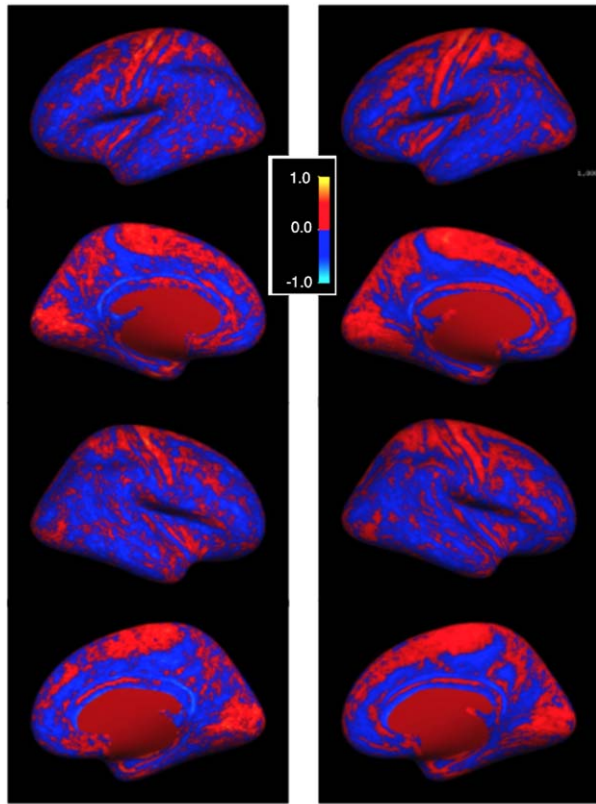
Whole cortex analysis of T1w/T2w ratio maps using 2-sample t tests showed a significant difference between the MS and HC groups for the left (MS vs HC, mean \pm SD: 0.720 ± 0.06 vs 0.739 ± 0.06 , $p = 0.02$) and right hemispheres (MS vs HC, mean \pm SD: 0.740 ± 0.06 vs 0.763 ± 0.06 , $p = 0.008$). Analogous measures of cortical thickness were significantly lower in the MS than in the HC group in the left (MS vs HC, mean \pm SD: 2.37 ± 0.10 mm vs 2.41 ± 0.10 mm, $p = 0.0005$) and right hemispheres (MS vs HC group, mean \pm SD: 2.37 ± 0.09 mm vs 2.42 ± 0.10 mm, $p = 0.0003$). Regional, that is, vertexwise, comparison of the MS and HC groups by a general linear model showed significantly lower T1w/T2w ratio values primarily in parietal and occipital areas (Fig 2), spreading into parts of the frontal and temporal lobe (superior temporal, pericentral, paracentral). After changing the significance threshold from 0.05 FDR-corrected to the more conservative threshold of $p = 0.00001$ uncorrected, 4 clusters remained. These clusters were located in the left and right medial occipital cortex mainly in the primary visual area (left: $\times = -6.5$, $y = -78.2$, $z = 6.3$, size = $1,611 \text{ mm}^2$; right: $\times = 11.3$, $y = -77.0$, $z = 6.0$, size = $2,308 \text{ mm}^2$), and in the left and right posterior cingulate cortex (left: $\times = -5.4$, $y = -28.2$, $z = 26.1$, size = 223 mm^2 ; right: $\times = 6.8$, $y = -19.2$, $z = 27.6$, size = 219 mm^2).

To test whether the decrease of the T1w/T2w ratio is functionally relevant, we correlated the values of the most prominent clusters with clinical scores. The posterior cingulate is assumed to play a central role for internally directed cognition, retrieval of memory, and attention,³⁶ which are in part covered by our clinical scores (see Table 2). Because correlation between the cluster values of the left and right posterior cingulate cortex was high ($R^2 = 0.7$) and because we had no hypothesis on lateralized effects, we used the individual mean values (collapsed across hemispheres) of both clusters for correlation with the 12 clinical scores given in Table 2. Of the 12 correlation analyses performed, 3 were nominally significant ($p < 0.05$) and another 2 showed a trend ($p < 0.1$). All 5 correlations were directed as hypothesized, that is, lower T1w/T2w ratio values went along with lower performance or more severe symptoms. Of note, the correlation with retrieval of wordlist B survived Bonferroni correction for multiple tests (see Table 2). The results of these correlation analyses were robust, as significance remained as described after extending the simple correlations to partial correlations by including age, global cortical thickness, and WM lesion volume as nuisance variables.

Validation analyses of the T1w/T2w ratio maps demonstrated the expected behavior. Group-averaged T1w/T2w ratio maps showed a heterogeneous distribution across the cortex. Of note, these maps very much resembled those reported recently,¹² with increased values in the primary areas (ie, visual cortex, auditory cortex, somatosensory strip), the paracentral lobule, and posterior cingulate cortex for both the MS and HC groups (see Fig 2A, B). We further analyzed whether T1w/T2w ratio values increase with age, as previously reported.^{15,18} The analysis of the relation between age and T1w/T2w ratios across the cerebral cortex showed a significant positive correlation in both groups (HC left hemisphere: $R = 0.31$, $p = 0.0053$; HC right hemisphere: $R = 0.31$, $p = 0.0052$; MS left hemisphere: $R = 0.21$, $p = 0.0004$; MS right hemisphere: $R = 0.19$, $p = 0.0016$). ANOVA did not indicate a significant interaction between group and age. Finally, we analyzed the correlation between cortical thickness and the T1w/T2w ratio in a vertexwise manner across all subjects, separately for each group. The correlation maps of both groups (HC and MS) showed that there is substantial variance in the relation between the two measures across regions with positive and negative correlations (Fig 3), indicating independence of the two measures.

Postmortem MRI and Histopathology

Although generated from patients in late stage secondary progressive MS, the average T1w/T2w ratio map of



Healthy controls

Multiple sclerosis patients

FIGURE 3: Relation between cortical thickness and T1/T2-weighted ratio values across the cerebral cortex. Surface maps of Pearson coefficients derived from vertexwise correlation analyses for the healthy control and multiple sclerosis groups are shown. Both groups display positive (red) and negative (blue) correlations across different cortical regions. Vertexwise Pearson coefficients are color-coded according to the bar (blue = negative correlations; red = positive correlations).

postmortem MRI (Fig 4) showed the highest values of the lateral cortex in the somatosensory strip similar to HC¹² and patients in early stages of MS (see Fig 2). Analysis of the T1w/T2w ratio yielded a significant relation to dendrite density ($p = 0.0008$), whereas the measures of myelin density, axonal density, and cortical thickness did not show even a trend (Fig 5). As this result was inconsistent with our primary hypothesis that the cortical T1w/T2w ratio reflects myelin, we performed control analyses. By another GEE, we observed the expected highly significant relation ($p < 10^{-9}$) between the histology-based and MRI-based measurement of cortical thickness (see Fig 5). Furthermore, all tissue blocks were once more thoroughly reviewed with a particular focus on myelin and dendrite stainings. The visual impression of the observer (L.E.J., J.J.G.G.) complied with the results of the GEE. An example of 1 patient is given in Figure 6.

T1w/T2w Ratio of the Posterior Cingulate Cortex across Groups In Vivo and Postmortem

The average images of all groups suggested that the preponderance of posterior areas with regard to the MS-related decrease of the T1w/T2w ratio continues to later disease stages. This visual impression was confirmed by plotting the scaled averaged values of the ROI of the posterior cingulate across all groups (Fig 7) and by group-wise t tests (HC in vivo vs MS in vivo: $p < 10^{-7}$; MS in vivo vs MS postmortem: $p = 0.12$; HC in vivo vs MS postmortem: $p = 0.02$).

Discussion

To the best of our knowledge, this is the first study to investigate cortical pathology in MS by analysis of the T1w/T2w ratio from conventional MRI both in vivo and postmortem. In vivo, we found a widespread decrease in posterior cortical areas and a positive correlation with attention in the posterior cingulate cortex. Postmortem MRI and histopathology demonstrated a significant relation of the T1w/T2w ratio to dendrite density. We will discuss the results of our in vivo data, consider technical issues related to the T1w/T2w ratio maps, and finally reflect on the results derived from our postmortem data, which challenge the idea that T1w/T2w ratio maps can be regarded as myelin maps.

In vivo, we observed lower T1w/T2w ratios in early stages of MS compared to HC. The effect was significant and showed a preponderance of posterior areas, in particular of the medial occipital cortex and the posterior cingulate cortex. We did not expect a preponderance of certain cortical regions. Yet by other MRI sequences,

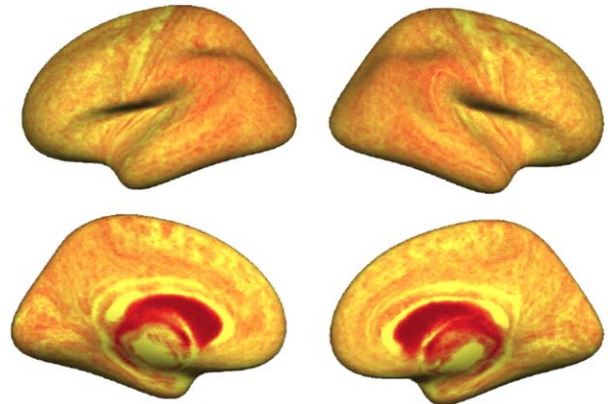


FIGURE 4: Average T1/T2-weighted (w) ratio maps from postmortem magnetic resonance imaging (MRI). The average surface map of cortical T1w/T2w ratio values, derived from postmortem MRI of 9 patients, is scaled from dark red for low values to light yellow for high values. The somatosensory strip shows the highest values of the lateral cortex. The overall signal distribution shows a preponderance of low values in posterior areas.

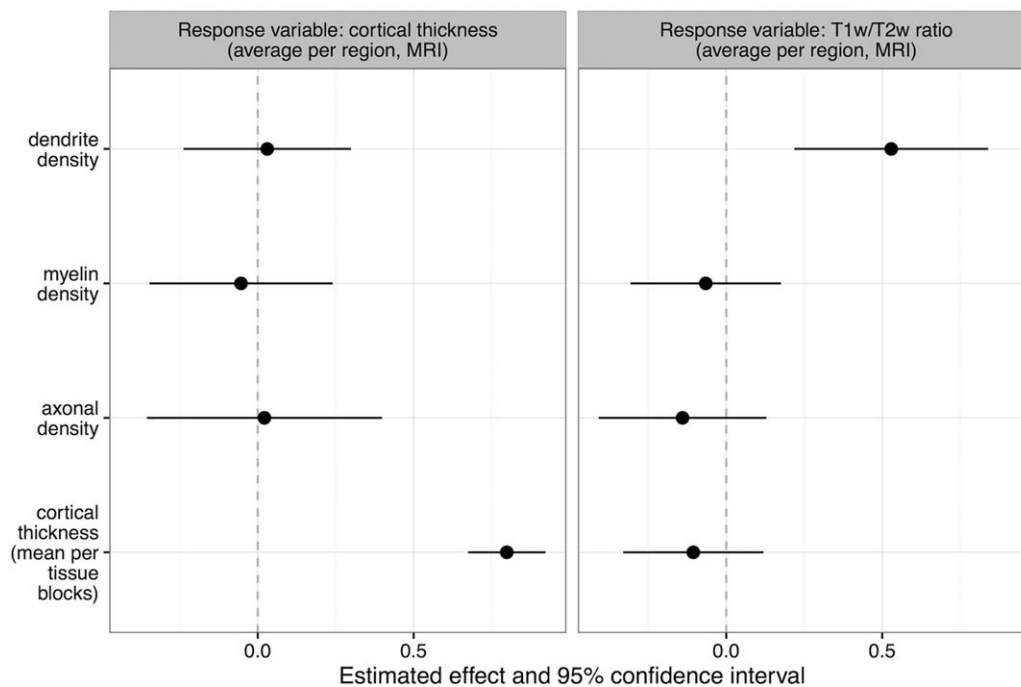


FIGURE 5: Histopathological measures and the T1/T2-weighted (w) ratio. Displayed are estimated effect sizes, directionality, and 95% confidence intervals of the influence of histology-based explanatory variables on the 2 magnetic resonance imaging (MRI)-based response variables of cortical thickness and T1w/T2w ratio. Values were derived from 4 separate general estimating equations (GEEs) per response variable, resulting in a total of 8 GEEs. In the control analyses (left panel), only histologically measured cortical thickness significantly correlated with MRI-based cortical thickness. Analysis of the T1w/T2w ratio (right panel) yielded a significant relation only to dendrite density.

similar spatial patterns were observed in studies on GM pathology in MS. Analyzing brain GM of CIS patients in a voxelwise manner by MTR, one study revealed decreased values bilaterally in the primary visual cortex.³⁷ In another study on whole brain GM in relapsing–remitting as well as primary and secondary progressive MS, MTR reduction was reported in the medial occipital cortex, and in the posterior cingulate, similar to the spatial pattern observed in our study.³⁸ Although long established to investigate WM fibers, diffusion tensor imaging (DTI) measures were also used to analyze GM integrity. Early studies demonstrated changes in the distribution of DTI-based measures across the cortex cross-sectionally³⁹ and longitudinally.^{40,41} Voxel-based techniques revealed widespread changes in GM integrity, including the medial occipital and cingulate cortex. Furthermore, the posterior cingulate cortex was also found to be predominantly altered in MS by 2 more recent studies using pattern recognition of cortical atrophy⁴² and multilayer MTR.⁴³ Given the similarity of spatial patterns on the MS-related changes in GM integrity, it seems possible that cortical pathology is not evenly distributed across the brain; instead, predilection sites may exist that are similarly but not identically covered by different methods. Furthermore, our results support the idea that the T1w/T2w ratio signal reflects functionally relevant

changes of the cortex, because lower values in the posterior cingulate cortex were associated with decreased performance in an attention task also requiring set shifting. Currently, we cannot distinguish whether the relation is specific for MS or physiological, as MuSIC subscores were not determined in our HC group and none of the mean values of the MuSIC subscores differed significantly from those given in the original publication on MuSIC.²² Nevertheless, our finding corresponds with cognitive deficits in patients having suffered from damage to the posterior cingulate cortex.³⁶ This relation is commonly explained by the finding that the posterior cingulate cortex is an important hub in the default mode network, which is also altered in MS.^{44,45}

With regard to methodology, we did not find an indication that our *in vivo* T1w/T2w ratio maps differed from those reported in the literature. The average T1w/T2w maps of HC and patients in early stages showed higher values in the somatosensory strip and in early auditory areas, as described before.¹² We also observed an age-related signal increase, as described before.^{15,18} Furthermore, correlations of the T1w/T2w ratio with cortical thickness varied greatly across the cortex, with both positive and negative correlations, so that cortical thickness does not systematically influence the T1w/T2w ratio as estimated in this study. Nevertheless, we cannot

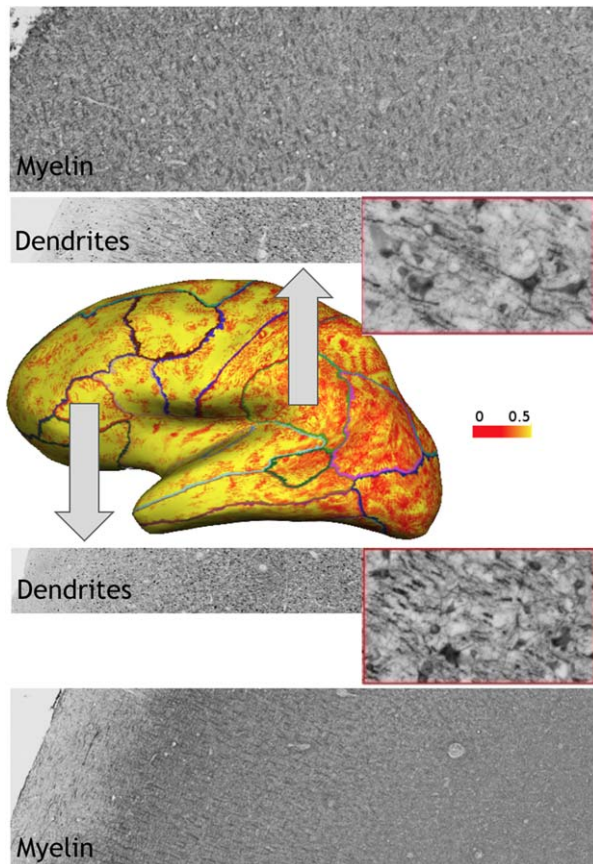


FIGURE 6: T1/T2-weighted (w) ratio map from postmortem magnetic resonance imaging (MRI) with corresponding dendrite and myelin staining. T1w/T2w ratio map from postmortem MRI and histopathology of Patient 5 are shown. The left lateral view on the T1w/T2w ratio map (scaled from dark red for low values to light yellow for high values) with the borders of cortical parcellations according to the Aparc atlas demonstrates high values within anterior regions, including the inferior frontal gyrus, and low values within posterior regions, including the inferior parietal gyrus. For both regions, corresponding dendrite (anti-microtubule associated protein 2) and myelin (anti-proteolipid protein) stainings are displayed. The insets on the right demonstrate higher dendrite density in the inferior frontal gyrus and lower dendrite density in the inferior parietal gyrus well in correspondence with the T1w/T2w ratio map. In contrast, myelin density was almost equal in both regions (inferior frontal gyrus, 0.248; inferior parietal gyrus, 0.264).

fully exclude that, despite manual correction of WM topology, cortical and juxtacortical lesions influenced cortical thickness and hence T1w/T2w ratio estimation to some degree. We applied rather strict quality criteria, which led to the exclusion of about 10% of the patients. Thus, at this stage of development, the T1w/T2w ratio method seems challenging for therapeutic trials and clinical practice, although both sequences are broadly available. However, exclusion of the whole MRI from analysis because of inaccurate registration of T1w and T2w images or because of a single problematic region with

regard to the identification of the cortical ribbon does not seem unsurmountable, but requires methodological development. Moreover, establishing the T1/T2 ratio as a biomarker of disease evolution or even treatment response in MS necessitates studies on changes over time of this parameter.

Processing of postmortem MRI data was more challenging because of the 3mm slice thickness of the T2w sequence, which may have introduced imprecision into our T1w/T2w ratio values. In addition, severe atrophy impeded sufficiently precise coregistration of the T1w and T2w images in 2 cases even after changing the settings of the FreeSurfer software. This left 9 postmortem MRI datasets for analysis. Given the late stage of MS, we did not expect to identify a certain spatial pattern. However, the average T1w/T2w ratio map showed higher values in the somatosensory strip, resembling the average T1w/T2w ratio maps reported so far^{15,18} and resembling the average T1w/T2w ratio maps of our in vivo data. Finally, we investigated whether T1w/T2w ratio values in the posterior cingulate cortex are lower in late stage MS compared to patients at earlier stages and to HC. This comparison was critical, as in vivo MRI and postmortem MRI were analyzed together. To address this issue, we scaled the T1w/T2w ratio values of the posterior cingulate cortex with the individual average across the whole

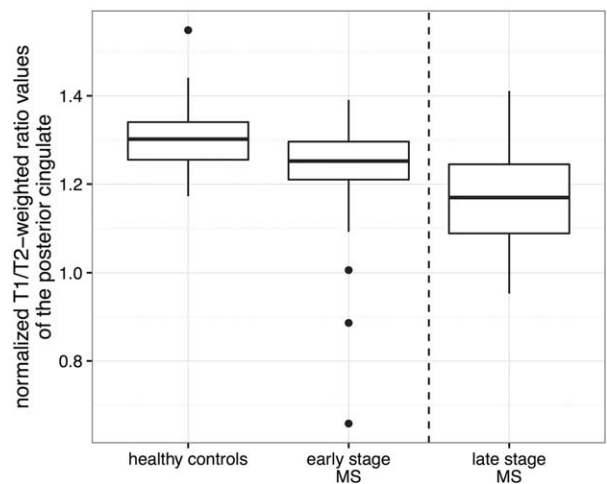


FIGURE 7: Normalized T1/T2-weighted (w) ratio values of the posterior cingulate in vivo and postmortem. Displayed are whisker plots of normalized T1w/T2w ratio values derived from the posterior cingulate. This region of interest (ROI) was derived from the 2 clusters of the group comparison of healthy controls and multiple sclerosis (MS) patients (see Fig 2D). All vertex values of this ROI were averaged for each subject and normalized by dividing them by the mean of all individual vertex values. T1w/T2w values decrease consistently from healthy controls to the early stage and to the late stage of MS, although magnetic resonance imaging of late stage MS was acquired postmortem with different technology (broken vertical line).

cortex. After this normalization, the T1w/T2w ratio values of the posterior cingulate cortex showed the hypothesized descending order from HC to early MS to late MS, compatible with the notion that the preponderance of the decrease of the T1w/T2w ratio in the posterior cingulate cortex continues in later disease stages.

Postmortem MRI and histological data gave us the rare opportunity to search for the histopathological substrate of the T1w/T2w ratio. To ensure that tissue blocks sufficiently overlapped with the MRI-based regions selected by the FreeSurfer cortical parcellation atlas *Aparc*, we performed a control analysis with the measure of cortical thickness determined by surface-based MRI as well as by histology. We found a highly significant relationship between both measures, indicating that our postmortem data are suitable to detect relations between MRI-based and histology-based measures. Such a relation was found. Dendrite density was the only parameter significantly driving the T1w/T2w ratio. At first glance, this may be surprising, as myelin density has been assumed to drive this signal. This assumption is based on the view that myelin is almost certain to drive the T1w signal of cerebral WM, because myelin maturation during brain development is perfectly paralleled by the T1w signal change from hypo- to hyperintense.²⁴ Furthermore, MRI-based T1w/T2w ratio maps resembled early histology-based myelin maps by Hopf so convincingly that MRI-based T1w/T2w ratio maps have also been termed "myelin maps."^{12–15,18,25} This evidence, however, is exclusively based on visual comparisons and, hence, indirect. Unfortunately, analogous histology-based maps of dendrite density do not exist, to the best of our knowledge. Thus, it is currently impossible to compare myelin density maps and dendrite density maps with regard to their degree of similarity to the T1w/T2w ratio maps. This would be of particular interest, given that differences in myelin density across cortical areas are commonly attributed to different functional roles of these cortical areas, that is, functional segregation. Unsurprisingly, the myeloarchitectonic maps by Hopf have overt similarities with the cytoarchitectural maps of Brodmann, and it is tempting to speculate that this would also apply to dendrite density maps. At this point, we acknowledge the limitation that we could only relate the MRI to histology in late stage MS brain donors and that this may not apply to cohorts of younger subjects *in vivo*. Ideally, future projects should investigate the association of the T1w/T2w ratio with dendrite density in brain donors without a neurological disease and in early stages of MS. Conversely, our results raise the question of evidence for dendrite pathology in MS. Such evidence exists. Although not surrounded by oligodendrocytes, transected

dendrites occur in both demyelinated and myelinated cortex.¹¹ A recent study revealed a widespread and pronounced loss of dendritic spines in MS cortex independent of cortical demyelination and axon loss.² The latest evidence using combined MRI and histopathology suggests that, in principle, the DTI-based measures of the cortex can reflect dendrite pathology,^{46,47} which is a possible explanation for the widespread changes of DTI-based measures in the cortex of MS patients.^{30,39–41}

In summary, we demonstrated a decrease of the T1w/T2w ratio in MS following a distinct spatial pattern. It was mainly located in posterior cortical areas, correlated with clinical scores, and seemed to reflect primarily dendrite pathology. Given its broad availability, the T1w/T2w ratio method is a promising candidate to study MS-related cortical pathology *in vivo*.

Acknowledgment

This work was funded by the Hertie Foundation (P1140092) and supported by the German Competence Network Multiple Sclerosis (German Ministry for Research and Education, 01GI1604A). B.H. was supported by the German Research Foundation (SFB TR-128).

Author Contributions

R.R., B.H., J.J.G.G., and M.M. contributed to the conception and design of the study. R.R., V.B., L.E.J., R.K., P.S., D.B., A.B., J.S.K., C.Z., and M.M. participated in the acquisition and analysis of data. R.R., V.B., L.E.J., P.S., B.H., J.J.G.G., and M.M. contributed to drafting the text or preparing the figures.

Potential Conflicts of Interest

Nothing to report.

References

1. Bo L, Geurts JJ, van der Valk P, et al. Lack of correlation between cortical demyelination and white matter pathologic changes in multiple sclerosis. *Arch Neurol* 2007;64:76–80.
2. Jürgens T, Jafari M, Kreutzfeldt M, et al. Reconstruction of single cortical projection neurons reveals primary spine loss in multiple sclerosis. *Brain* 2016;139:39–46.
3. Kutzelnigg A, Lucchinetti CF, Stadelmann C, et al. Cortical demyelination and diffuse white matter injury in multiple sclerosis. *Brain* 2005;128:2705–2712.
4. Lucchinetti CF, Popescu BF, Bunyan RF, et al. Inflammatory cortical demyelination in early multiple sclerosis. *N Engl J Med* 2011;365:2188–2197.
5. Filippi M, Evangelou N, Kangarlu A, et al. Ultra-high-field MR imaging in multiple sclerosis. *J Neurol Neurosurg Psychiatry* 2014;85:60–66.
6. Chen JT, Easley K, Schneider C, et al. Clinically feasible MTR is sensitive to cortical demyelination in MS. *Neurology* 2013;80:246–252.

7. Seewann A, Kooi EJ, Roosendaal SD, et al. Postmortem verification of MS cortical lesion detection with 3D DIR. *Neurology* 2012; 78:302–308.
8. Nelson F, Datta S, Garcia N, et al. Intracortical lesions by 3T magnetic resonance imaging and correlation with cognitive impairment in multiple sclerosis. *Mult Scler* 2011;17:1122–1129.
9. Roosendaal SD, Moraal B, Pouwels PJ, et al. Accumulation of cortical lesions in MS: relation with cognitive impairment. *Mult Scler* 2009;15:708–714.
10. Calabrese M, Romualdi C, Poretto V, et al. The changing clinical course of multiple sclerosis: a matter of gray matter. *Ann Neurol* 2013;74:76–83.
11. Peterson JW, Bo L, Mork S, et al. Transected neurites, apoptotic neurons, and reduced inflammation in cortical multiple sclerosis lesions. *Ann Neurol* 2001;50:389–400.
12. Glasser MF, Van Essen DC. Mapping human cortical areas in vivo based on myelin content as revealed by T1- and T2-weighted MRI. *J Neurosci* 2011;31:11597–11616.
13. Glasser MF, Coalson TS, Robinson EC, et al. A multi-modal parcellation of human cerebral cortex. *Nature* 2016;536:171–178.
14. Nieuwenhuys R, Broere CA. A map of the human neocortex showing the estimated overall myelin content of the individual architectonic areas based on the studies of Adolf Hopf. *Brain Struct Funct* 2016;222:465–480.
15. Grydeland H, Walhovd KB, Tamnes CK, et al. Intracortical myelin links with performance variability across the human lifespan: results from T1- and T2-weighted MRI myelin mapping and diffusion tensor imaging. *J Neurosci* 2013;33:18618–18630.
16. Leray E, Yaouanq J, Le Page E, et al. Evidence for a two-stage disability progression in multiple sclerosis. *Brain* 2010;133:1900–1913.
17. Polman CH, Reingold SC, Banwell B, et al. Diagnostic criteria for multiple sclerosis: 2010 revisions to the McDonald criteria. *Ann Neurol* 2011;69:292–302.
18. Shafee R, Buckner RL, Fischl B. Gray matter myelination of 1555 human brains using partial volume corrected MRI images. *Neuroimage* 2015;105:473–485.
19. Kurtzke JF. Rating neurologic impairment in multiple sclerosis: an expanded disability status scale (EDSS). *Neurology* 1983;33:1444–1452.
20. Cutter GR, Baier ML, Rudick RA, et al. Development of a multiple sclerosis functional composite as a clinical trial outcome measure. *Brain* 1999;122(pt 5):871–882.
21. Beck AT, Steer RA, Brown GK. *Manual for the Beck Depression Inventory-II*. San Antonio, TX: Psychological Corporation, 1996.
22. Calabrese P, Kalbe E, Kessler J. *Das Multiple Sklerose Inventarium Cognition (MUSIC)*. *Psychoneuro* 2004;30:384–388.
23. Yildiz M, Tettenborn B, Radue EW, et al. Association of cognitive impairment and lesion volumes in multiple sclerosis—a MRI study. *Clin Neurol Neurosurg* 2014;127:54–58.
24. Barkovich AJ. Concepts of myelin and myelination in neuroradiology. *AJNR Am J Neuroradiol* 2000;21:1099–1109.
25. Nieuwenhuys R. The myeloarchitectonic studies on the human cerebral cortex of the Vogt-Vogt school, and their significance for the interpretation of functional neuroimaging data. *Brain Struct Funct* 2013;218:303–352.
26. Dale AM, Fischl B, Sereno MI. Cortical surface-based analysis. I. Segmentation and surface reconstruction. *Neuroimage* 1999;9:179–194.
27. Fischl B, Dale AM. Measuring the thickness of the human cerebral cortex from magnetic resonance images. *Proc Natl Acad Sci U S A* 2000;97:11050–11055.
28. Greve DN, Fischl B. Accurate and robust brain image alignment using boundary-based registration. *Neuroimage* 2009;48:63–72.
29. Schmidt P, Gaser C, Arsic M, et al. An automated tool for detection of FLAIR-hyperintense white-matter lesions in multiple sclerosis. *Neuroimage* 2012;59:3774–3783.
30. Lulufiu S, Martinez-Heras E, Fortea J, et al. Cognitive functions in multiple sclerosis: impact of gray matter integrity. *Mult Scler* 2014;20:424–432.
31. Popescu V, Klaver R, Versteeg A, et al. Postmortem validation of MRI cortical volume measurements in MS. *Hum Brain Mapp* 2016; 37:2223–2233.
32. Popescu V, Klaver R, Voorn P, et al. What drives MRI-measured cortical atrophy in multiple sclerosis? *Mult Scler* 2015;21:1280–1290.
33. Destrieux C, Fischl B, Dale A, Hagren E. Automatic parcellation of human cortical gyri and sulci using standard anatomical nomenclature. *Neuroimage* 2010;53:1–15.
34. Geurts JJ, Roosendaal SD, Calabrese M, et al. Consensus recommendations for MS cortical lesion scoring using double inversion recovery MRI. *Neurology* 2011;76:418–424.
35. Klaver R, Popescu V, Voorn P, et al. Neuronal and axonal loss in normal-appearing gray matter and subpial lesions in multiple sclerosis. *J Neuropathol Exp Neurol* 2015;74:453–458.
36. Leech R, Sharp DJ. The role of the posterior cingulate cortex in cognition and disease. *Brain* 2014;137:12–32.
37. Audoin B, Fernando KT, Swanton JK, et al. Selective magnetization transfer ratio decrease in the visual cortex following optic neuritis. *Brain* 2006;129:1031–1039.
38. Mallik S, Muhlert N, Samson RS, et al. Regional patterns of grey matter atrophy and magnetisation transfer ratio abnormalities in multiple sclerosis clinical subgroups: a voxel-based analysis study. *Mult Scler* 2014;21:423–432.
39. Bozzali M, Cercignani M, Sormani MP, et al. Quantification of brain gray matter damage in different MS phenotypes by use of diffusion tensor MR imaging. *AJNR Am J Neuroradiol* 2002;23: 985–988.
40. Oreja-Guevara C, Rovaris M, Iannucci G, et al. Progressive gray matter damage in patients with relapsing-remitting multiple sclerosis: a longitudinal diffusion tensor magnetic resonance imaging study. *Arch Neurol* 2005;62:578–584.
41. Rovaris M, Judica E, Gallo A, et al. Grey matter damage predicts the evolution of primary progressive multiple sclerosis at 5 years. *Brain* 2006;129:2628–2634.
42. Steenwijk MD, Geurts JJ, Daams M, et al. Cortical atrophy patterns in multiple sclerosis are non-random and clinically relevant. *Brain* 2016;139:115–126.
43. Rudko DA, Derakhshan M, Maranzano J, et al. Delineation of cortical pathology in multiple sclerosis using multi-surface magnetization transfer ratio imaging. *Neuroimage Clin* 2016;12:858–868.
44. Rocca MA, Valsasina P, Absinta M, et al. Default-mode network dysfunction and cognitive impairment in progressive MS. *Neurology* 2010;74:1252–1259.
45. Richiardi J, Gschwind M, Simioni S, et al. Classifying minimally disabled multiple sclerosis patients from resting state functional connectivity. *Neuroimage* 2012;62:2021–2033.
46. Jespersen SN, Leigland LA, Cornea A, Kroenke CD. Determination of axonal and dendritic orientation distributions within the developing cerebral cortex by diffusion tensor imaging. *IEEE Trans Med Imaging* 2012;31:16–32.
47. Molet J, Maras PM, Kinney-Lang E, et al. MRI uncovers disrupted hippocampal microstructure that underlies memory impairments after early-life adversity. *Hippocampus* 2016;26:1618–1632.